Geogr. Fis. Dinam. Quat.
28 (2005), 7-21, 12 figg., 2 tabb.

KURT L. FRANKEL (*) & FRANK J. PAZZAGLIA (**)

TECTONIC GEOMORPHOLOGY, DRAINAGE BASIN METRICS, AND ACTIVE MOUNTAIN FRONTS

ABSTRACT: FRANKEL K.L. & PAZZAGLIA F.J., *Tectonic geomorphology, drainage basin metrics, and active mountain fronts*. (IT ISSN 1724-4757, 2005).

We use the gradients of first order channels and the ratio between drainage basin planimetric area and volume (R_{VA}) as primary topographic measures capable of distinguishing the relative tectonic activity of mountain fronts in both extensional and compressional tectonic settings. Here we report results from test cases on five mountain fronts with variable rates of rock uplift and deformational style in the western United States and Italy. Our study is guided by initial results obtained from two ranges in the southern Rocky Mountains, USA, Sierra Nacimiento and the Taos Range, that have departed on unique landscape developmental pathways related to the degree of tectonic activity on the range front fault. A frequency distribution of Taos Range and Sierra Nacimiento first order channel gradients is distinctly bimodal and the R_{VA} positively co-vary with tectonic activity for the Taos Range. We are able to generally reproduce these results for the tectonically active range front faults of the Wasatch Range in Utah and the Black Range in Death Valley, California. We also examined the relationship between R_{VA} and channel gradients for the foreland flank of the northern Apennines, Italy. A similar, positive relationship between R_{VA} and channel gradient exists in this fold and thrust belt, however these data exhibit higher variance than those collected from the uplifted footwall blocks in the western United States. We attribute the higher variance to the effects of overall larger drainage basin size investigated and the considerable variability in rock-type. In general, R_{VA} among the studied mountain fronts can be interpreted primarily in terms of the tectonic setting, and secondarily in terms of specific variations in drainage basin shape controlled by local rock-type and climatic setting. The R_{VA} is an effective metric in determining the relative tectonic activity of fault-bounded mountain fronts and escarpments. When combined the gradients of first-order streams, the R_{VA} can help determine the relative position of a catchment along a time-dependent drainage basin development curve.

KEY WORDS: Mountain fronts, Escarpments, Landscape metrics, Stream gradients, Landscape evolution.

INTRODUCTION

An argument can be made that the origins of modern tectonic geomorphology can be traced back to an interest in the relative activity of mountain fronts or escarpments known to be bounded by a normal fault (e.g. Bull & McFadden, 1977). Since erosion works to dissect and embay escarpments, Bull & McFadden (1977) reasoned that the linearity of mountain fronts and ratios of valley floor width to valley height should positively correlate with increased rates of rock uplift along a range bounding fault. This idea is well grounded in the general principles of geomorphology, so when differences in rock-type and climate can be minimized, the Bull & McFadden (1977) classification of relative tectonic activity has proven to be an effective tool in the quantitative analysis of tectonically active landscapes (Rockwell & *alii*, 1985; Gardner & *alii*, 1987; Wells & *alii*, 1988). Advances in the quality, acquisition, and processing of high- resolution digital topography over the past decade has enabled geomorphologists to rapidly, quantitatively, and more objectively interpret topography in terms of tectonic processes. Digital topography, when coupled with independent measures of both uplift and erosion rates can fully investigate the core hypotheses first forwarded in the Bull & McFadden approach (Pazzaglia & Brandon, 1996; Brown & *alii*, 2002; Matmon & *alii*, 2002).

There exists a class of mountain fronts and escarpments that generally mimic the morphology of active fault-bounded escarpments because of recent, rapid exhumation and juxtaposition of hard and soft rock types. In a new paper, Frankel & Pazzaglia (2006) defined a suite of new metrics, easily measured from high resolution digital elevation models in a GIS that help distinguish between erosionally exhumed landforms and escarpments bounded by an active fault. The more traditional metrics of mountain front sinuosity and valley floor width to valley height ratios, which do a relatively poor job in separating the exhumed from active fault-bounded mountain fronts are replaced by measurements of first-order stream gradients and the average depth (the drainage basin volume to drainage basin area ratio) of

(*) *Department of Earth Sciences, University of Southern California - 3651 Trousdale Parkway, Los Angeles, CA 90089, USA.*

(**) *Department of Earth and Environmental Sciences, Lehigh University - 31 Williams, Bethlehem, PA 18015, USA.*

The core of this paper represents work of the first author's master's thesis at Lehigh University. Funding was provided by the Lehigh University Department of Earth and Environmental Sciences, the Colorado Scientific Society, the United States Geological Survey EDMAP program, and NSF grants EAR-0207980 (RETREAT project) and EAR- 9909393. We thank A. Densmore for early stimulating discussions and subsequent formal review and R. Arrowsmith for a second, very helpful review of the manuscript.

transverse valleys. Initial results from an application of this approach to two diverse mountain fronts in New Mexico, U.S.A. are promising (fig. 1; Frankel & Pazzaglia, 2006), but the hypothesis and methodology require further testing.

This paper returns to the roots of topographic-based tectonic geomorphology to quantify the characteristics of mountain fronts that are currently being shaped by active tectonics. Our approach uses the first-order stream gradient and drainage basin volume to drainage basin area ratio metrics extracted from high-resolution digital elevation models and explores mountain fronts undergoing active deformation in a wide range of climatic, lithologic, and tectonic settings. We hypothesize, based on numerous field studies, analogue models, and numerical simulations that first order stream gradients and drainage basin volume to drainage basin area ratio metrics are relatively insensitive to rock type and climate at the orogen scale and rather, prove to be a first-order quantification of the relative tectonic activity for mountain fronts. We discover a general confirmation of our method; however, the role of rock type and climate, even over broad regions, can impart a control on landscape development that remains difficult to separate from the effect of tectonics alone.

LANDSCAPE DEVELOPMENT OF ESCARPMENTS

Escarpments can form anytime there is a juxtaposition of rock types of variable resistance to erosion, from base level fall and the resulting headward migration of an exhumational wave front (Humphrey & Heller, 1995; Zaprowski & *alii*, 2001; Garcia & *alii*, 2003), or when a fault emerges at the Earth's surface and actively displaces one block of crust with respect to another. Offset along a fault

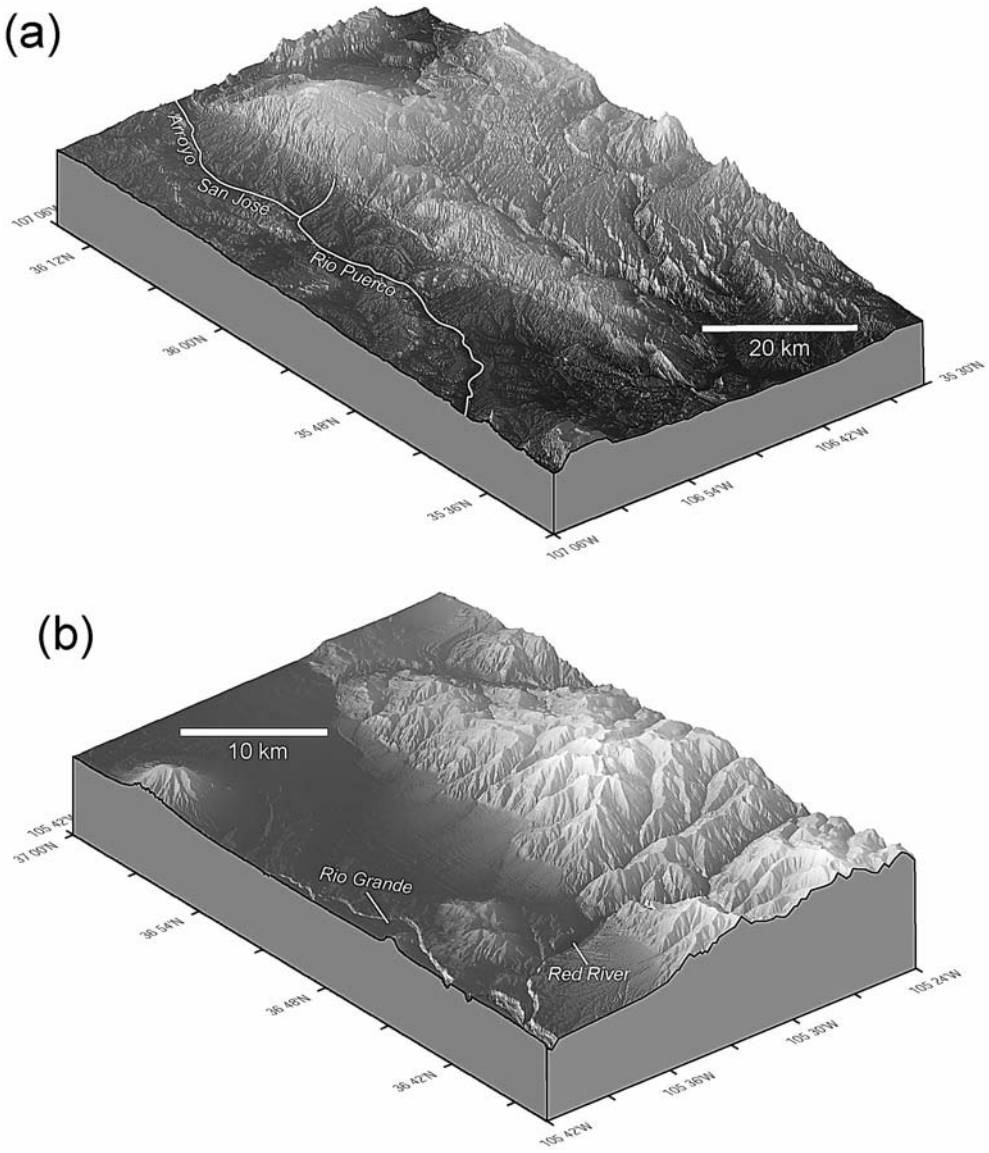

FIG. 1 - Contrasting topography of (a) Sierra Nacimiento, a mountain front bounded by an inactive range-front fault and (b) the Taos Range, a mountain front bounded by an active range front fault. The overall shape of the drainage basins and hillslopes reflect the low frequency of landslides on the relatively gentle slopes of Sierra Nacimiento in contrast to the higher frequency of landslides in the Taos Range.

has the effect of producing a local base level fall. Once formed, escarpments tend to persist because of the spatial segregation of fluvial and erosional processes linked to mean hillslope gradient and drainage area (Bryan, 1940; King, 1953; van der Beek & *alii*, 2002). Much of our current understanding of escarpment erosional dynamics comes from studies of Great Escarpments on passive margins (Ollier, 1985; Tucker & Slingerland, 1994; Kooi & Beaumont, 1994; Gilchrist & *alii*, 1994; Beaumont & *alii*, 2000; Bishop & Goldrick, 2000; Brown & *alii*, 2000; Cockburn & *alii*, 2000); however, we apply the general model that has emerged from these studies of large-scale landforms to the smaller-scale escarpments formed by offset along an active normal fault.

Early ideas suggesting escarpments experience only parallel retreat with river valleys eroding headward at the same rate as interfluves (King, 1953) have been tempered by contemporary studies that argue for rapid erosion at the foot of escarpments early in their history, nucleation of the escarpment at or near its current location, and the subsequent significant slowing of erosional processes (Brown & *alii*, 2000, 2002; Bierman & Caffee, 2001). This is particularly true when there is an isostatic feedback between erosion and flexural bending of the crust, such that drainage divides remain fixed on the crest of the escarpment (Tucker & Slingerland, 1994; Matmon & *alii*, 2002). In this manner, escarpments of ancient origin along passive margin settings have not undergone significant parallel retreat, but instead have experienced only minor modification because the rates of erosion have decreased significantly since their formation. In these tectonically stable settings, there is a long lag time between the formation of the escarpment and denudation response that ultimately tears it down.

In contrast, tectonically active settings have fast erosion rates because rock uplift is countered by rapid stream incision, which keeps mean hillslope angles steep. In this case, the lag time between the formation of the escarpment and its erosion is short. The Bull & McFadden (1977) approach, as well as the approach we adopt in this study is predicated on the assumption that landscape response times are fast in tectonically active regions, thereby allowing erosion to respond in pace with rock uplift.

There are a plethora of morphometric variables that have been proposed as sensitive to active tectonics (e.g. Wells & *alii*, 1988) along mountain front escarpments, but the goal of this paper is not to test their relative applicability to our study area. Rather, we embark on an examination of two simple metrics, one that has clearly been linked to the rate of rock uplift, and the other that has clearly been observed to change in response to base level fall as drainage basins develop in analogue models.

THE DRAINAGE BASIN VOLUME TO AREA RATIO (R_{VA}) AND STREAM GRADIENTS

Numerous analogue studies have shown the mean depth of transverse catchments is sensitive to the rate of base level fall (e.g. Schumm & *alii*, 1987), yet few studies have fully explored this metric in real landscapes. We express this mean depth as:

$$R_{VA} = \frac{V}{A} \qquad (1),$$

where V is the volume of a drainage basin in m^3 and A is the planimetric area of a drainage basin in m^2. Drainage basin size and shape is known to vary as a function of time, given similar substrate, climate, and rate of base level fall (Glock, 1931; Morisawa, 1964; Parker & Schumm, 1982; Ritter & Gardner, 1993; Ouchi & Matsushita, 1997; Hasbargen & Paola, 2000; Bonnet & Crave, 2003; Lague & *alii*, 2003; Densmore & *alii*, 2005). R_{VA} is one measure of how the mean depth of the basin changes through time and is crudely equivalent to basin hypsometry (Strahler, 1952; Pike & Wilson, 1971) and the valley excavation index (Harbor, 1997). Most analogue studies run their experiments under an impulsive or steady fall in base level designed to mimic episodic or continuous rock uplift. A base level forcing mechanism of initial accelerating fall, followed by steady fall is shown on fig. 2 as the gray, dashed curve. The erosional response to this base level fall is plotted as the R_{VA} and the general shape of this curve is very similar to what has been directly observed in terms of sediment yield in analogue models with this type of base level fall forcing (Bonnet & Crave, 2003).

The relationship between R_{VA} and sediment yield as erosion proceeds in a growing drainage basin deserves further inspection. In fig. 2, both R_{VA} and sediment flux would be expected to grow in pace with one another through stage 2 during the time that the catchment is widening and deepening and hillslopes are steep. Sediment flux and R_{VA} reach maximum values at stage 3 where R_{VA} can be maintained indefinitely as long as rock uplift continues and erosion can keep pace with uplift. However, both analogue and numeric

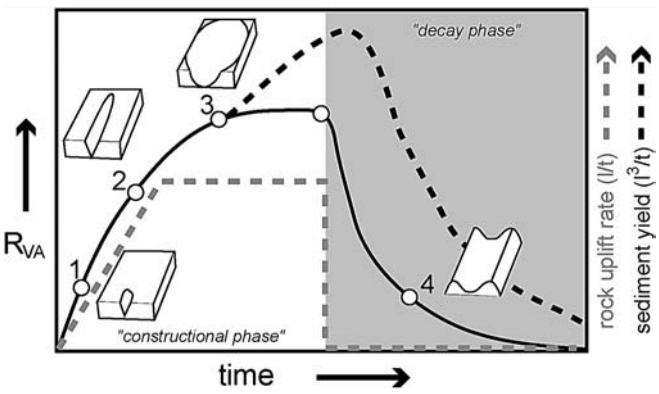

FIG. 2 - General development of drainage basin shape with respect to time, showing the predicted change in the average depth of the basin, in meters, expressed as the ratio of drainage basin volume to planimetric area (R_{VA}). Drainage basin erosion is assumed to proceed in response to a base level fall at the mouth of the basin expressed as a rate of rock uplift (gray axis to the right where l = units of length and t = units of time). The rate of rock uplift is initially rapid and accelerating, then becomes constant, and finally ceases.

models predict that sediment flux should become independent of R_{VA} at stage 3 as it keeps pace with rates of base level fall (rock uplift) (Densmore & *alii*, 1998; Roering & *alii*, 1999, 2001). In other words, when hillslopes reach a critical threshold angle, and drainage basins have attained a steady state relief and mean depth, R_{VA} ceases to change, but sediment yield varies by the rate that the hillslopes are failing. When hillslopes throughout the drainage basin are shallower than ~20 degrees, sediment flux is linearly proportional to hillslope gradient. Once hillslopes steepen above ~20 degrees, landsliding becomes an important process and sediment flux is non-linear with respect to slope. At the threshold hillslope condition, there may be no relationship between hillslope gradient and sediment yield (Montgomery & Brandon, 2002). Because of this, erosion rates and sediment flux can vary significantly during stage 3, however the R_{VA} is shown to approach a maximum value and remains more or less constant until rock uplift ceases, at which point, R_{VA} decays.

The assumption that R_{VA} approaches a maximum value is based on empirical data we have explored from diverse digital elevation data sets, studies that support uniform basin widths and spacing on uplifted footwall blocks (Densmore & *alii*, 2005), and analogue models (Hasbargen & Paola, 2000; Bonnet & Crave, 2003; Lague & *alii*, 2003). We can construct a simple geometric model to illustrate the point. Numerous factors influence the average depth of a drainage basin. Most notably are the basin shape, drainage density, overall gradient of the trunk stream profile, and average hillslope gradient. Of these, the mean hillslope gradient is perhaps the most important because it controls the relief between the valley floor and encompassing divides. Representative ranges in the R_{VA} as a function of mean hillslope angle and average basin width can be calculated assuming simple drainage basin geometry and a reasonable gradient for the trunk channel. We start with a model drainage basin with a rectangular planimetric shape and a fixed length of 10 km oriented transverse to a mountain front escarpment. We model variable widths of 2, 4, and 6 km for this basin. These widths correspond to an escarpment 8, 16, and 24 km in length respectively, dimensions that are well within the range of observed drainage basin sizes and spacing in uplifted footwalls of active normal faults (Hovius, 1996; Densmore & *alii*, 2005). We note however, that the shape of the real basins is typically not rectangular like our model basin but are rather elliptical or oval. Next, a single, straight trunk stream is placed in the center of the basin and allowed to excavate a valley into an imaginary box below the rectangular planimetric form. The mouth of the stream exits the box at one end where there is a free boundary. The head of the stream ends at a no flow boundary defined as a vertical wall connecting the opposing divides parallel to the stream. We assign a constant gradient to the drainage basin hillslopes (α) in degrees, such that the trunk stream has two smooth, opposing hillslopes stretching from the drainage divide to the channel. The hillslope angle and drainage basin width define the relief of the opposing divides. From this simple geometry, it is easy to construct an uncorrected drainage basin volume (V_{uc}) in cubic meters from the drainage cross sectional area (A_{cs}) in square meters, the drainage width (W) in meters, and the drainage length (L) in meters where:

$$A_{cs} = 2(0.125)[\tan(\alpha)(W)][W] \quad (2),$$

and

$$V_{uc} = (Acs)(L) \quad (3).$$

We correct the calculated volume by accounting for the gradient of the trunk channel. We assume a gradient of the trunk channel such that its headwaters against the no-flow boundary are 25% higher than it is at its mouth:

$$V = 0.75V_{uc} \quad (4).$$

The corrected drainage basin volume is then divided by the planimetric area to calculate the R_{VA} (fig. 3).

Our simple model predicts that tectonically inactive landscapes, presumably those with low mean hillslope angles, will mostly have R_{VA} values less than 100, whereas tectonically active landscapes, presumably those with high mean hillslope angles, will have R_{VA} values greater than 100 (fig. 3). Insofar that a drainage basin's mean hillslope angle represents an equilibrium form, that is, the opposing divides are lowering as fast as the stream is incising, then the R_{VA} for that drainage basin will be a fixed value. Studies in tectonically active areas have argued that hillslope angle is insensitive to rates of rock uplift when the rates of rock uplift are high enough to create hillslopes at the critical angle of failure, typically with distributions around 30 degrees (Burbank & *alii*, 1996). Fig. 3 predicts that for a given catchment width, there should be a theoretical maximum value for the R_{VA} set by the threshold hillslope angle. The maximum R_{VA} value for drainage basins spanning the

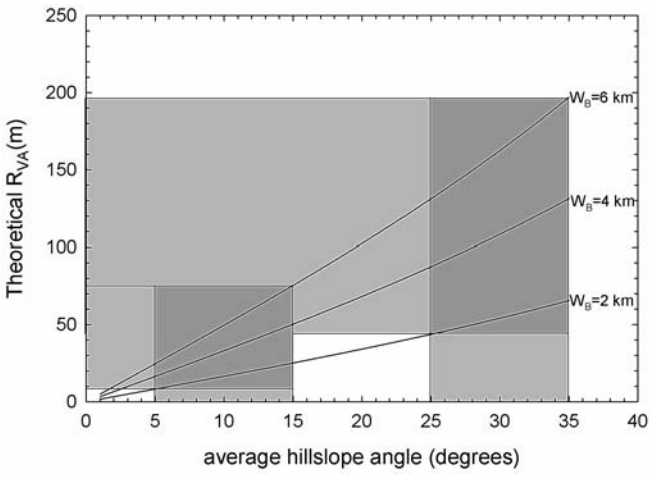

FIG. 3 - The R_{VA} as a function of mean hillslope angle in a simple, theoretical basin shaped like an inverted triangular prism, with one open end, and a second closed, no flow boundary. Tectonically inactive mountain fronts generally have R_{VA} values less than 100 m whereas tectonically active mountain fronts have a wider range of R_{VA} values that are usually greater than 100 m. Threshold hillslope angles around 30 degrees define an upper limit for R_{VA} values, depending on the average width of the drainage basin. W_B = basin width.

wide range of areas modeled here (5-200 km^2) lies between approximately 100 m and 200 m.

The R_{VA} for exhumed and tectonically active mountain fronts are known to be different for at least one study where rock type and climate are known to be constant (fig. 1; Frankel & Pazzaglia, 2006). R_{VA} values for the exhumed mountain front range from 74 m to 109 m with a mean value of 88 m whereas the values for the tectonically active mountain front range from 89 to 180 m with an average of 140 m. Sensitivity testing of the method using basins in other tectonically active settings show that for drainages spaced approximately 5 km apart (5 km mean widths), the maximum R_{VA} lies in the range of 180 to 200 m, in good agreement with the predictions of fig. 3.

Nevertheless, fig. 2 shows a non-unique dependence of the R_{VA} with respect to time (stages 2 and 4 in fig. 2), reinforcing the point that we need other data to help distinguish the position of drainage basins on the R_{VA} vs. time curve. One source of complementary data that can be obtained easily and directly from digital topography, and does not suffer the same problems of sediment yield for the steady-state landscape is the gradient of stream channels. Rates of rock uplift and opposing rates of river incision are known to be reflected in the gradients of stream channels; primarily in the gradients of low-order channels (Merritts & Vincent, 1989). A wide distribution of steep channels, especially low order channels, would be expected to plot on the growing to steady-state parts of the curve in fig. 2. In contrast, uniformly gentle channels would be expected to plot on the decaying part of the curve in fig. 2. Consequently, we use both the R_{VA} and first-order stream gradients to describe drainage basin development for our study areas.

STUDY AREAS AND METHODOLOGY

Gradients of first order channels (S_{1ord}) are measured following the methodology similar to that of Merritts & Vincent (1989). First order channel gradients of the uplifted range block and approximately 5 km of adjacent piedmont were extracted from 10 and 30 meter resolution digital elevation models in Arc/Info. The channels were defined by a flow accumulation threshold with a drainage area of 0.025 km^2. This resulted in a subsequent ordering of the entire drainage basin stream network, similar to that which would be obtained from standard 1:24,000 scale topographic maps (Pazzaglia, 1989). First order channel long profiles were extracted as ASCII data from the DEM at 4.5 meter increments and these data were parsed using a FORTRAN code to calculate a gradient based on the minimum and maximum elevations in the long profiles. The channel gradients are then binned and plotted in a histogram to determine the mode.

The same high resolution DEMs and Arc/Info GIS are used to measure the R_{VA} (Frankel, 2002). First, individual drainage basins are extracted from the DEM by defining the catchment outlet at the range front. The DEM of each individual drainage basin was then resampled to 100 m. A maximum elevation envelope map is produced from the resampled data by interpolating a surface between local maximum elevations in a circular moving window with a 5 km radius. This allows the envelope maps to be pinned to the watershed divide and cover the maximum elevations within each drainage basin. Next, the maximum elevation maps are resampled back to the original DEM resolution so that the true topography can be subtracted from the envelope surface. Subtracting the original DEM from the maximum elevation envelope map produces a topographic residual raster that is then converted to a TIN, from which area and volume data can be extracted.

We investigate four mountain ranges with contrasting styles and rates of tectonic deformation. Three of these areas are located in the western United States and one is located in northern Italy (fig. 4). In the western United States, we compile first-order stream gradient and R_{VA} values from the Taos Range and Sierra Nacimiento in northern New Mexico, the Wasatch Range in central Utah, and the Black Mountains in Death Valley, California (tab. 1).

TABLE 1 - Basic metrics of studied mountain ranges

Mountain Front	Length (km)	Width (km)	Mean relief (m)	Mean transverse drainage spacing (km)	Range front fault slip rate (mm/yr)	Rock type	Mean annual precipitation (cm/yr)
Sierra Nacimiento	80	10-16	611	4.6	0[a]	Proterozoic granite and gneiss[f]	40-112[k]
Taos Range (segment 1)	35	22-27	836	1.12	0.1-0.5[b]	Proterozoic granite and gneiss[g]	40-91[k]
Wasatch Range (Weber segment)	34	11-17	1239	2.07	1-2[c]	Precambrian granite, Phanerozoic sedimentary cover, and Tertiary plutonic[h]	50-140[k]
Black Mountains	90	3-17	1518	2.37	1-3[d]	Precambrian crystalline basement and Paleozoic metasediments[i]	<6[k]
Northern Apennines	220	69-76	450	12.6	0.1–2[e]	tectonized Mesozoic and Tertiary marls, carbonates, basalts, and siliciclatic turbidites[j]	80-150[l]

[a] Frankel & Pazzaglia (2006); [b] Menges (1990a, b); [c] Matson & Bruhn (2001); [d] Klinger & Piety (2001); [e] Pazzaglia (unpublished data); [f] Woodward (1987); [g] Lipman & Reed (1989); [h] Bryant (1990); [i] Holm & Wernicke (1990); [j] Boccaletti & *alii*, 2004; [k] Western Region Climate Center (http://www.wrcc.dri.edu/); [l] Regione Emilia-Romagna (1995).

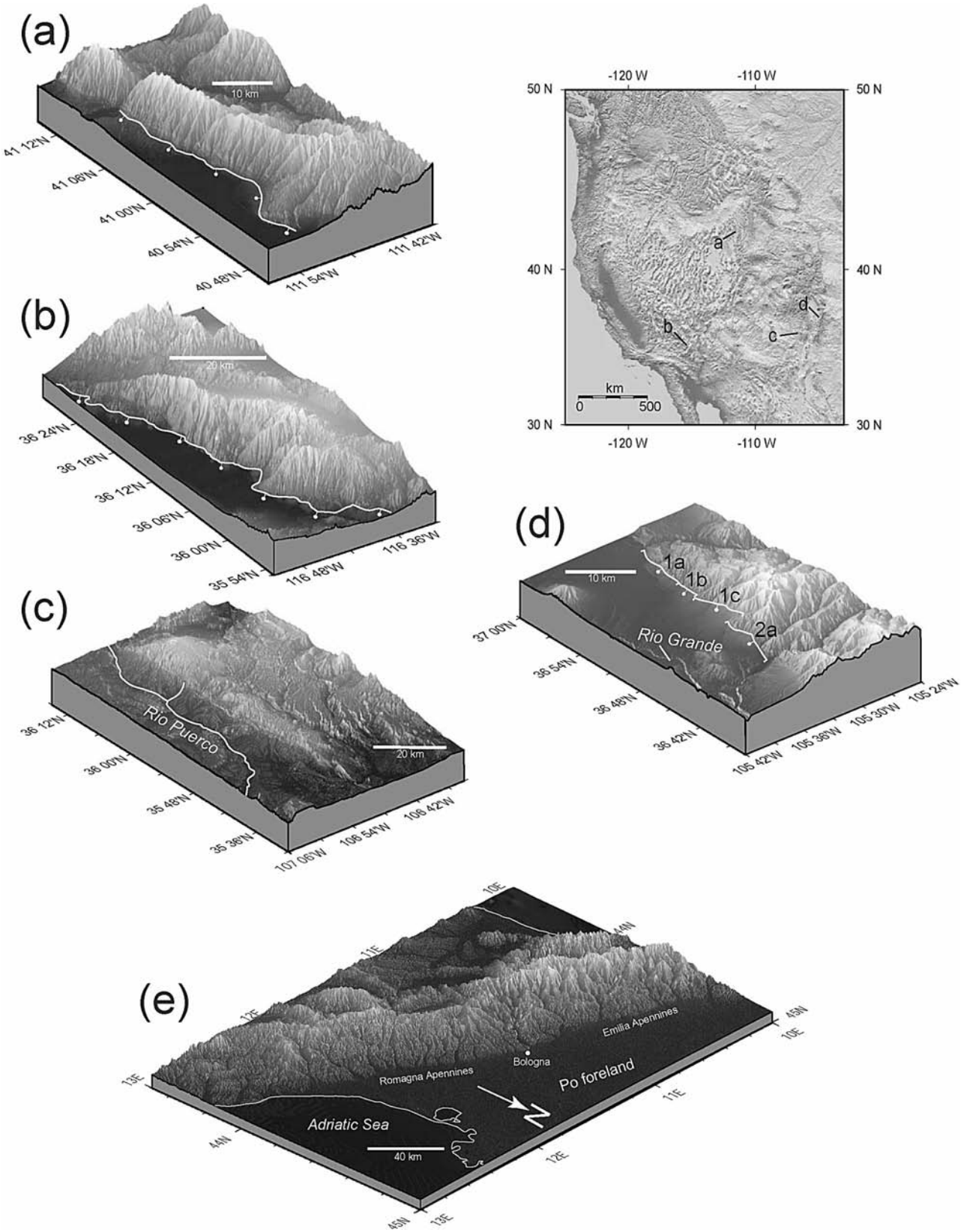

FIG. 4 - Geographical locations of the study areas in the western United States and northern Italy. (a) Wasatch Range, Weber segment, Utah; (b) Black Mountains, Death Valley, California; (c) Sierra Nacimiento, New Mexico; (d) Taos Range, northern segments, New Mexico; (e) northern Apennines and Po foreland.

Sierra Nacimiento is bounded to the west by an inactive, high-angle reverse fault along which the range was uplifted during the Laramide orogeny. The Black Mountains, Taos Range, and Wasatch Range are all bounded on their west sides by an active normal fault related to widespread crustal extension of the western U.S. from the Neogene to the present. The Quaternary slip rates on these faults show considerable overlap, but also tend to increase from zero for Sierra Nacimiento, ~0.1-0.5 mm/yr for segment 1 of the Taos Range (Menges, 1990a, b), 0.9-2 mm/yr for the Weber segment of the Wasatch Range (Machette & *alii*, 1991; Chang & Smith, 2002), and ~1-3 mm/yr for the Black Mountains (Klinger & Piety, 2001; Hayman & *alii*, 2003). More importantly, the range bounding fault of the Taos and Wasatch mountain fronts are segmented with known, variable Quaternary slip rates. Long-term exhumation rates of these footwalls are constrained by thermochronologic studies and range from 0.16-0.24 mm/yr for segment 1 of the Taos Range (Pazzaglia & Kelley, 1998) to 0.2-0.4 mm/yr for the Weber segment of the Wasatch Range (Armstrong & *alii*, 2004). The Black Mountains may also be segmented, but the precise slip rate of each segment is not yet known. Rates of late-Miocene to recent unroofing of the Black Mountains based on fission-track thermochronology range from 0.77-1.76 mm/yr (Holm & Dokka, 1993).

The relative size and relief of investigated mountain fronts are comparable (tab. 1); however, there are some notable differences in both rock type and climatic setting. Sierra Nacimiento and the Taos Range are underlain almost solely by Proterozoic granite and gneiss, with minor amounts of Phanerozoic sedimentary or volcanic cover rocks. The Wasatch Range has a mix of Precambrian crystalline rocks, Phanerozoic sedimentary cover, and Tertiary intrusive rocks. The Black Mountains are a mix of Precambrian crystalline rocks, Paleozoic carbonates and metasediments, intruded by Tertiary granitic plutons, and in places covered by a thin veneer of Pliocene and Quaternary sediments (Holm & Wernicke, 1990). Climate for Sierra Nacimiento, the Taos Range, and Wasatch Range is semi-arid to mountain-alpine. These ranges receive an elevation-dependent mean annual precipitation of 40 to 100 cm. The Black Mountains, in contrast, lie in a much more arid setting, receiving less than 6 cm of rainfall annually.

The northern Apennines, in contrast, are an uplifted forearc related to the subduction of the Adria microplate during general convergence of Europe and Africa. We investigated the northern flank of the range, which exposes a fold and thrust belt verging north towards the Po Plain (fig. 4). The mountain front itself makes both an abrupt and gentle transition to the Po Plain where there is local evidence for an active range-front fault (Benedetti & *alii*, 2003). With respect to the Po Plain, the entire fold and thrust belt is actively being uplifted at rates ranging from 0.1 to 2 mm/yr (Spagnolo & Pazzaglia, 2005; Pazzaglia, unpublished data). The western half of the studied range is capped by the Ligurian nappe structural lid, which represents the intact roof of a large passive roof duplex. These rocks are pervasively tectonized Mesozoic and Tertiary marls, with lesser amounts of carbonates and gabbro. During the Quaternary these rocks have been stripped away by erosion across the eastern half of the range where the underlying Miocene foredeep, composed of the Marnosa Arenacea siliciclastic turbidites, is exposed (Cerrina Feroni & *alii*, 2001). The implication is that the eastern half of the range and its mountain front has experienced significantly larger amounts of rock uplift during the Quaternary.

RESULTS

We measure S_{1ord} (fig. 5) and R_{VA} for the major transverse drainages along mountain fronts in the five study areas (tab. 2). The drainages generally range from 3rd to 5th order in size and reach all the way back to the watershed divide of the uplifted range block. There are a few smaller drainages particularly along the Taos Range mountain front that do not meet these size criteria and we discuss their S_{1ord} and R_{VA} values separately below. A collective plot of all S_{1ord} and R_{VA} values using R_{VA} as the independent variable shows covariance between these two metrics (fig. 6). There is no strong justification for using R_{VA} as the independent, rather than dependent variable and in this case, the results would be the same if the axes were reversed. A degree of auto correlation exists between R_{VA} and S_{1ord} because, as fig. 3 illustrates, the average hillslope angle determines the height of opposing watershed divides and hence the R_{VA}. Nevertheless, fig. 6 shows a clear distribution of data where mountain fronts experiencing relatively higher rock uplift rates also have the steepest first order streams and the highest values of R_{VA}. Insofar that the long-term rock uplift rate for the mountain fronts is linked to the slip rates on the range bounding faults, it would be useful to see how fault slip rate is related to R_{VA}. We have reliable data for fault slip rates for the Taos Range and Wasatch mountain fronts only, but both provide further support for the direct linkage between

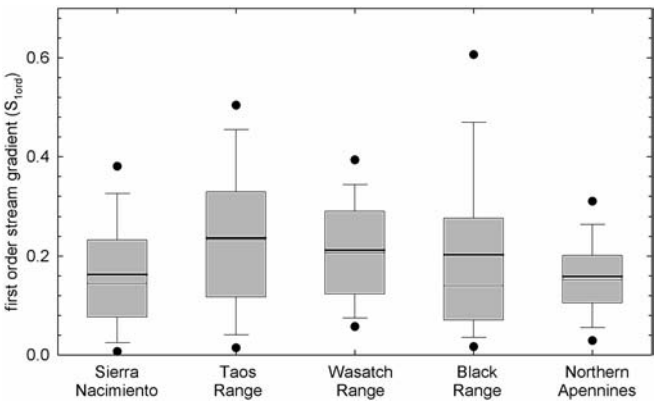

FIG. 5 - Box and whisker plot showing the S_{1ord} for investigated mountain fronts. The thin horizontal line is the median value, the thick horizontal line is the mean value, the boxes represent the 25th to 75th percentile, the whiskers represent the 10th and 90th percentile, and the dots represent the outliers as the 5th and 95th percentile.

TABLE 2 - Results of S_{1ord} and R_{VA} analyses

Mountain Range	Drainage Basin	Area (km^2)	S_{1ord} range (m/m)	S_{1ord} mean (m/m)	R_{VA} (m)
Sierra Nacimiento	Arroyo de los Pinos	3.1	0.12-0.31	0.22	109 ± 8
	Rito Olguin	3.6	0.05-0.36	0.20	81 ± 7
	Arroyo Dedos Gordos	3.6	0.07-0.32	0.20	75 ± 7
	San Pablo Canyon	25.6	0.04-0.26	0.15	80 ± 7
	Nacimiento Creek	10.7	0.04-0.18	0.11	77 ± 7
	La Jara Creek	14.0	0.06-0.32	0.19	74 ± 7
	Salado Creek	1.4	0.16-0.43	0.30	88 ± 7
	San Jose Creek	6.0	0.15-0.40	0.28	104 ± 8
	Senorito	10.6	0.07-0.22	0.15	102 ± 8
	San Miguel Canyon	13.1	0.06-0.28	0.17	93 ± 8
Taos Range	Jaracito Canyon	5.6	0.11-0.41	0.26	180 ± 10
	Latir Creek	36.0	0.08-0.39	0.23	139 ± 9
	Rito del Medio	12.6	0.13-0.43	0.28	156 ± 9
	Upper Sunshine East	1.2	0.14-0.36	0.25	133 ± 9
	Upper Sunshine NW	0.9	0.08-0.31	0.20	122 ± 8
	North Jaracito Canyon	3.7	0.09-0.56	0.32	141 ± 9
	Penasquito Canyon	1.6	0.08-0.25	0.16	89 ± 7
	Canada Pinabete	3.9	0.10-0.40	0.25	148 ± 9
	Rito Primero	12.9	0.14-0.44	0.29	174 ± 10
	South Rito Primero	0.8	0.29-0.37	0.33	118 ± 8
	North Penasquito Canyon	0.5	0.21-0.31	0.26	147 ± 9
	North Urraca Canyon	0.7	0.09-0.41	0.25	132 ± 9
	Urraca Canyon	8.2	0.12-0.41	0.26	139 ± 9
	Jaroso Basin	9.5	0.07-0.26	0.16	104 ± 8
	El Rito Canyon	1.0	0.05-0.48	0.27	180 ± 10
Wasatch Range	Mill Creek	28.6	0.003 - 0.47	0.17	145 ± 9
	Holbrook Canyon	13.7	0.03 - 0.38	0.17	150 ± 9
	Ward Canyon	12.0	0.08 - 0.47	0.24	147 ± 9
	Centerville Canyon	8.9	0.05 - 0.32	0.23	150 ± 9
	Parrish Creek	5.9	0.07 - 0.31	0.18	138 ± 9
	Ford Canyon	7.0	0.14 - 0.53	0.32	153 ± 9
	Steed Canyon	7.0	0.17 - 0.56	0.32	176 ± 10
	Farmington Creek	29.3	0.01 - 0.29	0.13	149 ± 9
	Shepard Creek	6.1	0.18 - 0.38	0.26	197 ± 11
	Baer Creek	8.9	0.16 - 0.48	0.29	183 ± 10
	Holmes Creek	6.9	0.19 - 0.41	0.32	178 ± 10
	Holmes Creek North	5.7	0.08 - 0.41	0.26	195 ± 10
	Kays Creek South	4.2	0.31 - 0.55	0.33	188 ± 10
	Kays Creek North	3.1	0.10 - 0.49	0.29	166 ± 10
Black Mountains	Agnes	7.5	0.06 - 0.58	0.25	181 ±10
	Becky	5.4	0.18 - 0.8	0.36	247 ± 12
	Clementine	4.1	0.1 - 0.54	0.27	194 ± 10
	Dotty	6.3	0.08 - 0.30	0.17	202 ± 11
	Ernestine	1.7	0.03 - 0.92	0.50	196 ± 10
	Coffin Canyon	2.1	-	-	191 ± 10
	Sheep Canyon	30.3	0.01 - 0.17	0.20	195 ± 10
	Willow Creek	65.0	0.002 - 0.56	0.11	129 ± 9
	Mormon Point	6.4	0.03 - 0.87	0.31	161 ± 9
	Smith Mountain	7.0	0.03 - 0.78	0.35	186 ± 10
	South of Smith Mountain	5.9	0.44 - 0.56	0.52	225 ± 11
	Black Canyon	7.2	0.15 - 0.29	0.20	187 ± 10
	North Scotty's Canyon	10.4	0.11 - 0.21	0.17	172 ± 10
	Scotty's Canyon	15.4	0.01 - 0.17	0.12	135 ± 9
Northern Apennines	Taro	1663.0	0.002 - 0.69	0.18	94 ± 8
	Baganza	151.2	0.03 - 0.82	0.21	111 ± 8
	Parma	361.8	0.0007 - 0.40	0.16	104 ± 8
	Enza	526.2	0.001 - 0.52	0.16	106 ± 7
	Tresinaro	178.0	0.0004 - 0.2	0.09	76 ± 8
	Secchia	1136.2	0.0005 - 0.83	0.17	103 ± 8
	Panaro	1054.8	0.003 - 0.61	0.19	91± 8
	Reno	1143.6	0.0008 - 0.64	0.16	109 ± 8
	Santero	477.8	0.0008 - 0.67	0.13	98 ± 8
	Senio	266.9	0.001 - 0.23	0.08	103 ± 8
	Lamone	296.9	0.003 - 0.44	0.13	110 ± 8
	Montone	298.8	0.001 - 0.5	0.15	99 ± 8
	Rabbi	244.5	0.004 - 0.41	0.14	107 ± 8
	Ronco (Bidente)	485.2	0.002 - 0.52	0.15	119 ± 8
	Savio	957.2	0.007 - 0.44	0.13	93 ± 8

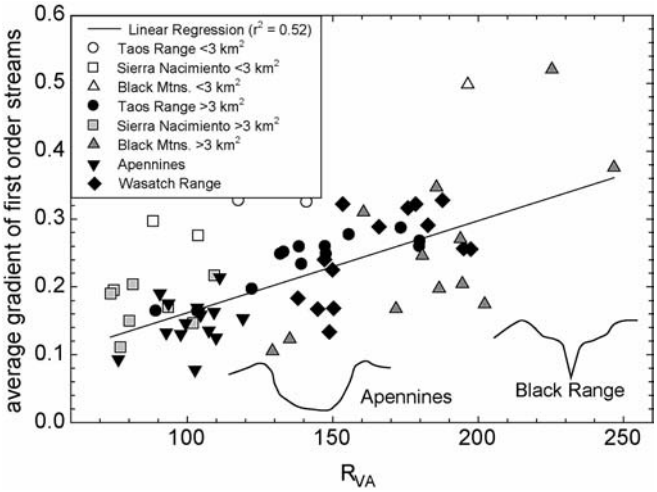

FIG. 6 - Plot of S_{1ord} against R_{VA} confirming the theoretical exercise of fig. 3 and demonstrating that R_{VA} is also a useful measure of relative tectonic activity for mountain fronts and escarpments. The sketches illustrate representative cross-section valley profiles (not to scale).

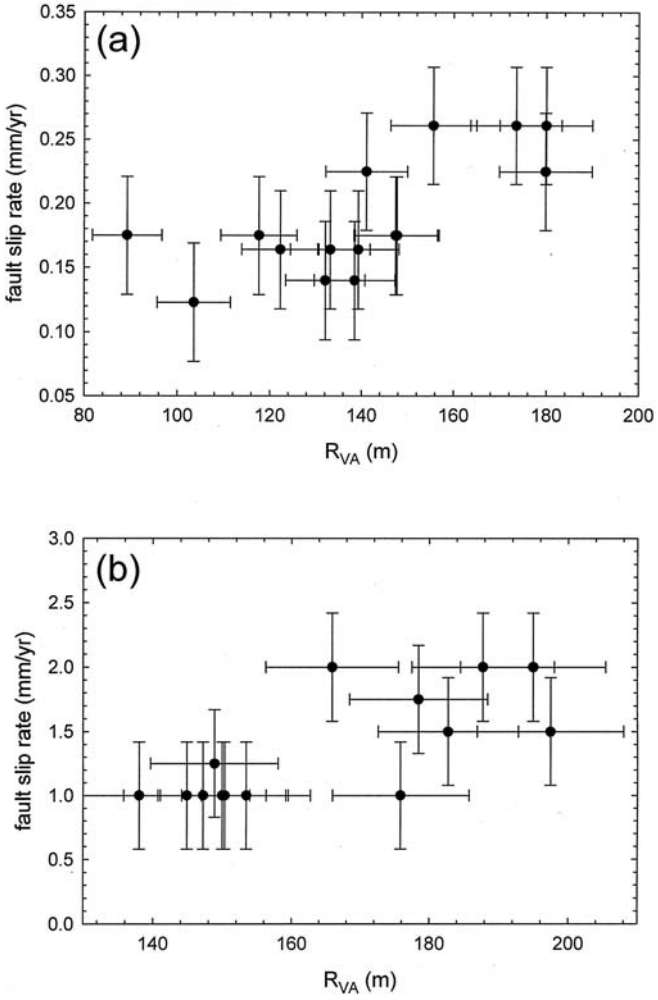

FIG. 7 - Range-bounding fault slip rate plotted against R_{VA} for the (a) Taos Range and (b) Wasatch Range. Error bars represent standard measurement error for R_{VA} and uncertainties in fault slip rates.

drainage basin shape, expressed as the R_{VA} and rate of rock uplift (fig. 7).

We can further investigate the relationship of S_{1ord} and R_{VA} by showing how these metrics plot spatially along the investigated mountain fronts (tab. 2). Starting with the tectonically inactive mountain front, Sierra Nacimiento, a plot of S_{1ord} and R_{VA} with respect to the position of where major transverse drainages exit the escarpment reveals relatively low values for both metrics, with a decrease in mean channel gradient from north to south, but no discernable along strike trend in R_{VA} (fig. 8). In contrast, plots of S_{1ord} and R_{VA} for the tectonically active, and segmented range front faults of the Taos Range and Wasatch Range show relatively higher values for each metric (figs. 9 and 10). More importantly, S_{1ord} and R_{VA} systematically increase for those fault segments that have been demonstrated to have relatively high fault slip rates. In the case of the Taos Range, fault segments in the north rupture less frequently than those in the south. Comparative mountain front landforms, such as facets are wide and gently-sloped in the north, and steep and narrow in the south (Menges, 1990a). Similarly, alluvial fans in the north are broad and gently sloped whereas those aligned along the southern segment are narrow and steep (Pazzaglia, 1989). In particular, the Taos Range R_{VA} values increase from north to south in concert with these other active tectonic metrics (fig. 9). In the Wasatch Range, it is the fault segments in the south that are less active than those in the north. In fact, this range stands as a case study in how mountain front landforms and metrics such as mean relief can be used to define fault segments (Schwartz & Coppersmith, 1986, c.f. Armstrong & *alii*, 2004). The Wasatch Range S_{1ord} and R_{VA} values systematically increase from the south to the north in agreement with increasing uplift rates along the northern segments and the related changes in mountain front landforms (fig. 10). There are a few notable outliers in the data plotted in figs. 9 and 10. For each one of these outliers, the drainage basin investigated was quite small (< 3 km^2) and not a true transverse drainage extending all the way back to the drainage divide in the interior part of the range.

The Black Mountains range front differs from the Taos and Wasatch ranges in that the R_{VA} values are generally larger and the S_{1ord} values show a wider variance, with some of the highest gradients measured for any of our study areas. Additionally, there is no clearly observable trend in either of these metrics along the mountain front (fig. 11). Insofar that segmentation of the Black Mountains has yet to be determined, all that can be summarized from these data is that they are commensurate with the overall rapid rates of uplift and low amounts of precipitation this range has experienced in the Quaternary. The drainage spacing in the Black Mountains is similar to that in the

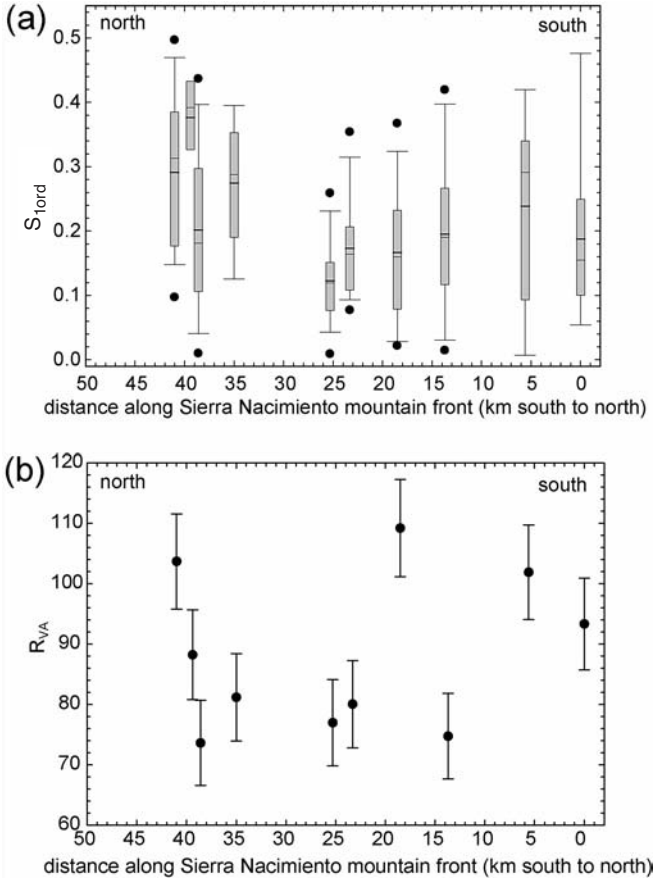

FIG. 8 - Plots of (a) S_{1ord} and (b) R_{VA} for the tectonically inactive Sierra Nacimiento mountain front. For (a) the thin horizontal line is the median value, the thick horizontal line is the mean value, the boxes represent the 25th to 75th percentile, the whiskers represent the 10th and 90th percentile, and the dots represent the outliers as the 5th and 95th percentile. For (b) error bars represent standard measurement error.

Taos and Wasatch ranges. Therefore, the consistently higher S_{1ord} and R_{VA} values point to drainage basins that are steeper and narrower.

The northern Apennine mountain front has S_{1ord} and R_{VA} values intermediate between the clearly tectonically active Taos, Wasatch, and Black ranges, and the tectonically quiescent Sierra Nacimiento (fig. 12). A plot of the S_{1ord} distributed along the mountain front shows a clear decrease to the east; however, there is no trend in the R_{VA} values, which tend to cluster around a value of 100 m. The length of the Northern Apennine mountain front, the size of the drainage basins, and the drainage basin spacing are all larger than the other escarpments investigated (tabs. 1, 2).

DISCUSSION AND CONCLUSIONS

Landforms and topographic metrics of mountain fronts continue to be a focal point in the application of tectonic geomorphology to answer questions regarding the relative activity of escarpments bounded by an active fault. Traditional measures of mountain front sinuosity and valley floor width to valley height ratios (Bull & McFadden, 1977), although useful, suffer several drawbacks in terms of their ability to distinguish active from inactive escarpments (Frankel & Pazzaglia, 2006). We propose a new metric tied to the average depth of transverse drainage basins along an escarpment that is a better measure of the relative activity of the bounding fault. This metric, which we call the drainage basin volume to drainage basin area ratio (R_{VA}) is easy to measure from widely available digital elevation models. Moreover, this metric is less subjective than other mountain front metrics in that there are less objective decisions on precisely what to measure. Variations in the R_{VA} have a firm grounding in a long history of drainage basin develop-

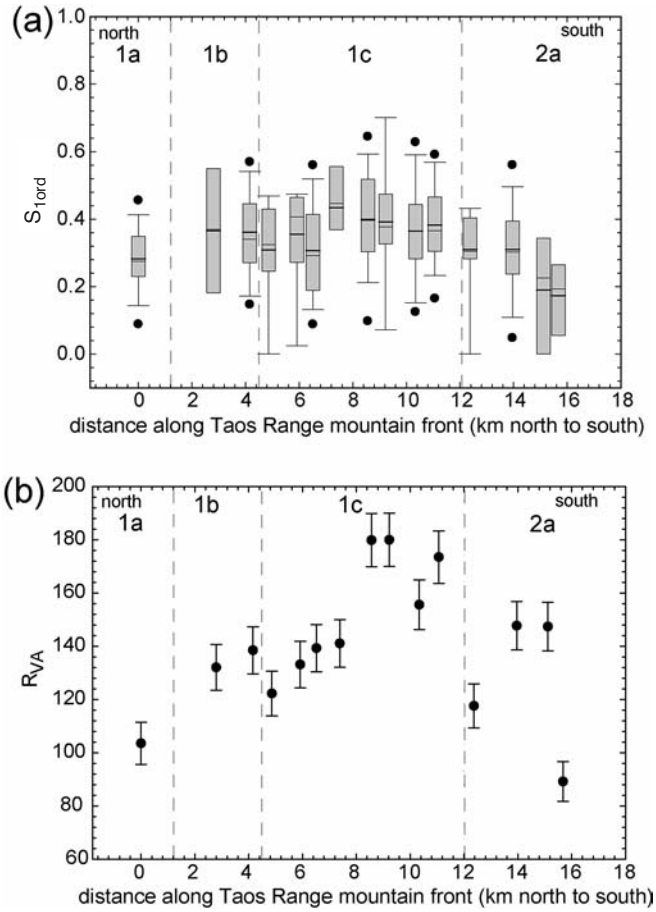

FIG. 9 - Plots of (a) S_{1ord} and (b) R_{VA}, for the tectonically active and segmented Taos Range mountain front. For (a) the thin horizontal line is the median value, the thick horizontal line is the mean value, the boxes represent the 25th to 75th percentile, the whiskers represent the 10th and 90th percentile, and the dots represent the outliers as the 5th and 95th percentile. For (b) error bars represent standard measurement error. Offset on fault segments increases from north to south. Segments are as defined by Menges (1990a, b).

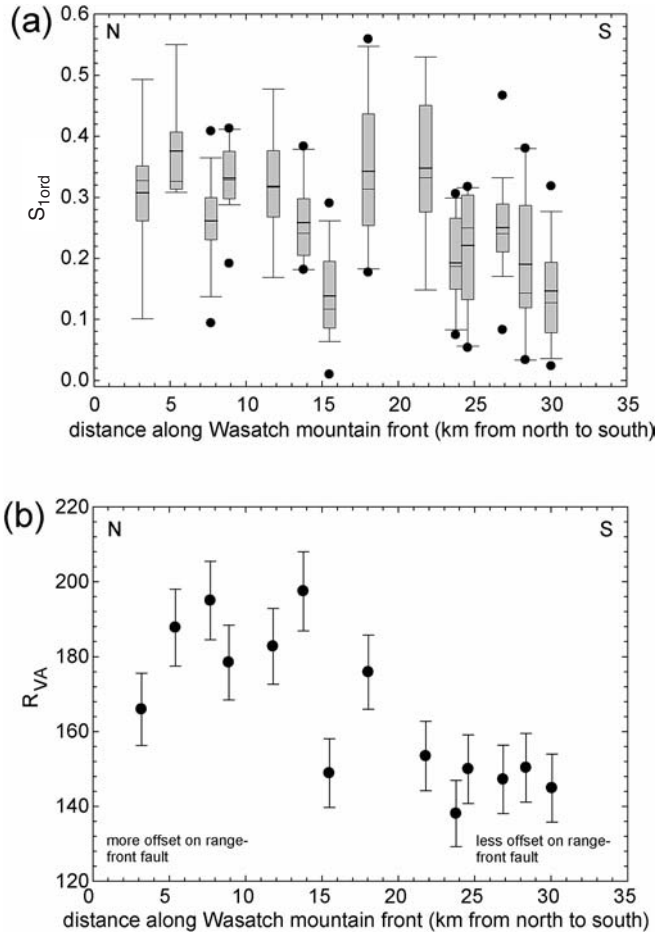

FIG. 10 - Plots of (a) S_{1ord} and (b) R_{VA} for the Weber segment of the tectonically active and segmented Wasatch Range mountain front. For (a) the thin horizontal line is the median value, the thick horizontal line is the mean value, the boxes represent the 25th to 75th percentile, the whiskers represent the 10th and 90th percentile, and the dots represent the outliers as the 5th and 95th percentile. For (b) error bars represent standard measurement error. Offset on the Weber segment of the Wasatch fault increases from south to north.

ment studies and when combined with other data such as sediment yield or stream gradients, can be used to identify a catchment's position on a time-dependent drainage basin development diagram (fig. 2). For our purposes, it is the distinction of drainage basins plotting between stages 2 and 3, as opposed to stage 4, on fig. 2 that allows us to determine the relative tectonic activity of a mountain front.

The strong correlation between the rate of rock uplift, first-order stream gradients, and R_{VA} for the Taos and Wasatch Ranges (figs. 6, 7, 9, and 10) is particularly convincing because the rock-type, climate, and style of deformation for these footwall blocks are all relatively similar. Contrary to the long-term exhumation rates of the Wasatch Range footwall, which records pre-Quaternary regional erosion rather than fault-generated relief of the modern escarpment, our data suggest that geomorphology does reflect the fault slip rates and segmentation pattern (c.f. Armstrong & *alii*, 2004). Perhaps not surprisingly, the scales of transverse drainage basins that have developed in the uplifted footwall block of the normal faults forming these ranges are also comparable. Similar results regarding the size, shape, relief, spacing, and eroded volume of material have been reached by other studies in the Basin and Range (e.g. Harbor, 1997; Densmore & *alii*, 2004). For segmented, normal-fault bounded ranges where the rock type is dominated by hard, crystalline basement or siliciclastic sedimentary rocks, R_{VA} alone distinguishes well between slow (≤ 0.1 mm/yr) and rapid (≥ 0.5 mm/yr) rates of rock uplift with corresponding R_{VA} values of ~100 m and approaching the quasi-steady state value of ~200 m respectively. We argue that the drainage basins in the most rapidly uplifting parts of the Taos and Wasatch ranges are at, or near,

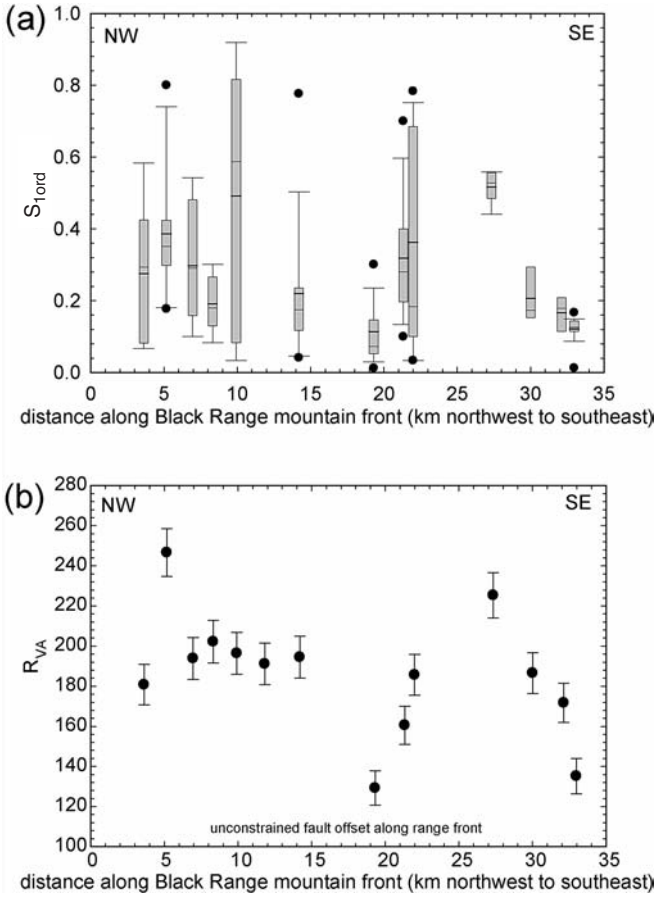

FIG. 11 - Plots of (a) S_{1ord} and (b) R_{VA}, for the tectonically active Black Mountains range front. For (a) the thin horizontal line is the median value, the thick horizontal line is the mean value, the boxes represent the 25th to 75th percentile, the whiskers represent the 10th and 90th percentile, and the dots represent the outliers as the 5th and 95th percentile. For (b) error bars represent standard measurement error. Fault segmentation has not been defined for this range front.

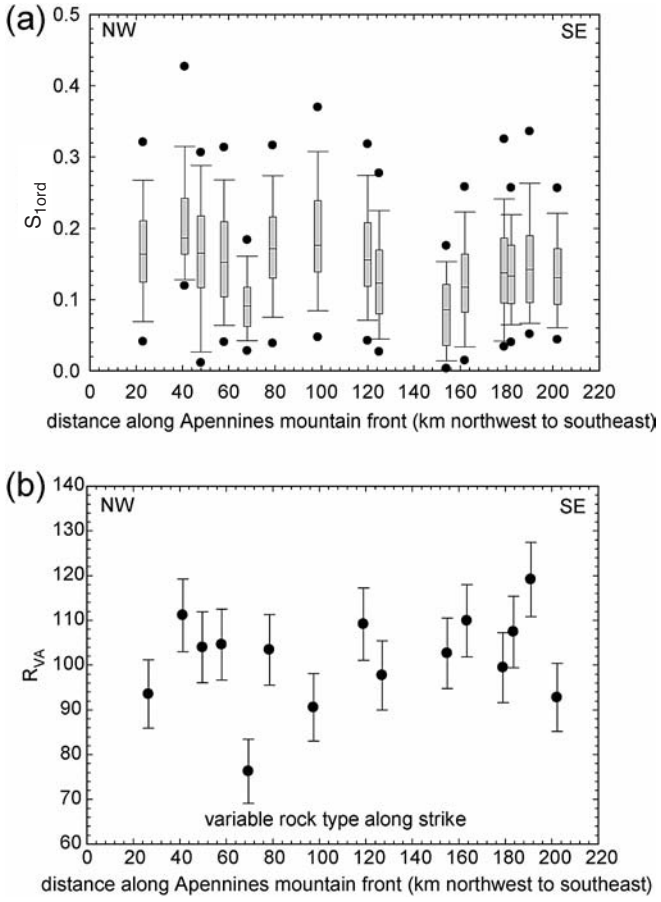

FIG. 12 - Plots of (a) S_{1ord} and (b) R_{VA} for the tectonically active northern Apennine mountain front. For (a) the thin horizontal line is the median value, the thick horizontal line is the mean value, the boxes represent the 25th to 75th percentile, the whiskers represent the 10th and 90th percentile, and the dots represent the outliers as the 5th and 95th percentile. For (b) error bars represent standard measurement error. Rock type is variable along strike.

steady state (position 3 in fig. 2). Catchments in these parts of the ranges are well adjusted to the rates of rock uplift along the active normal faults defining their respective escarpments.

In contrast, the generally higher S_{1ord} and R_{VA} values for the Black Mountains in Death Valley are a bit more difficult to interpret in terms of tectonics alone because of the change in climatic setting and rock type. Two-thirds of the Black Mountains basins have a relatively high R_{VA} and low S_{1ord} in comparison to the Taos and Wasatch Range data, which have equal numbers of basins on either side of the regression line in fig. 6. The S_{1ord} data is primarily collected from the periphery of the drainage basins so these results can be interpreted as showing that drainage basins in the Black Mountains have a rind of relatively gentle gradients surrounding the drainage divide, but valley axis streams are deeply incised and valleys are narrow. In cross-section, such a drainage basin would have a main valley with a wine-glass shape and this morphology is characteristic of catchments in the Black Mountains (sketch in fig. 6). We interpret this shape and R_{VA} values to indicate a drainage basin between stages 2 and 3 on fig. 2, still in a constructional stage of its development. This constructional stage implies some lag between the timing of rock uplift and the erosional response of the landscape, which may be related to fast uplift rates, or alternatively, relatively slow erosion influenced by rock type or the arid climate. Our analysis is not able to distinguish which factors are most important in this case.

Both Sierra Nacimiento and the northern Apennines have lower R_{VA} and S_{1ord} values than the Taos Range, Wasatch Range, or Black Mountains and these values occupy a small cluster on fig. 6. This cluster is expected for Sierra Nacimiento because it is a tectonically inactive escarpment where both the low S_{1ord} and R_{VA} values suggest that this is an erosionally exhumed mountain range undergoing topographic decay (Stage 4 in fig. 2; Frankel & Pazzaglia, 2006).

The northern Apennines, in contrast, are tectonically active, yet they show values of S_{1ord} or R_{VA} more similar to the tectonically inactive Sierra Nacimiento, keeping in mind all appropriate considerations for differences in rock type and climate. The style of deformation in the northern Apennines is different than the other ranges we investigated in that the mountain front is poorly defined by a blind or locally emergent reverse fault. In addition, rock uplift in the northern Apennines is regional and not simply concentrated across one structure defining the escarpment. This comparatively larger mountain range has, as expected, more widely-spaced transverse drainage basins, so theoretically it should contain some of the largest R_{VA} values (fig. 2). Instead, we find just the opposite. We interpret these seemingly contradictory results primarily in terms of rock type. Although the climate for the northern Apennines is not appreciably different than it is for large parts of the Great Basin in the western U.S., it is different enough such that given the exposed rock types, the dominant hillslope process tends to be large earthflows. These earthflows are particularly prevalent in the western portion of the northern Apennine study area and they have the effect of keeping the overall slopes in watersheds relatively low. The cross-sectional shape of the drainage basins are bowl-like and lack the narrow inner valleys of the Black Mountains, for example (inset sketch in fig. 6). The steeper S_{1ord} values for the western part of the northern Apennines support our suggestion of bowl-shaped catchments with steep sides, and are consistent with the fact that many of the low-order streams are developed on more resistant carbonate or siliciclastic units defining the drainage divides, rather than the soft rocks undergoing erosion by large earthflows. The eastern part of the northern Apennines have lower and rather uniform S_{1ord} values, which are consistent with the mean rock-type resistance and high drainage density resulting from the uniformly distributed siliciclastic tur-

bidites and valleys with flattened, parabolic cross-sections. We interpret the northern Apennines to be a range still in its constructional phase of development, at or near stage 2 on fig. 2. The particular shape of drainage basins in this region, during the constructional development phase, can be attributed to the rock-type and distributed nature of rock uplift.

Drainage basins that are relatively small (< 3 km^2) and not transverse to the entire mountain front in the Sierra Nacimiento, Taos Range, and Black Mountains have very steep stream gradients relative to their R_{VA} values (fig. 6). Such basins have low eroded volumes and the valley walls must be very steep all the way from the valley bottom to the drainage divide. In cross-section, these valleys would look similar to slot canyons. The fact that drainage basins of this shape are found on both tectonically active and inactive mountain fronts speaks to the fact that erosional lag time increases as drainage basin area decreases. In other words, it is difficult for small drainage basins with ephemeral discharge to respond to a base level fall, regardless of whether it is tectonically or exhumationally induced. An analogous scenario is glacially-formed hanging valleys. We interpret the small drainage basins in our study to be caught somewhere between stages 1 and 2 of fig. 2, and not able to progress further until tectonic or climatic conditions change, allowing them to grow, or to be captured and incorporated into a larger transverse drainage. We caution against using drainage basins that do not extend to the drainage divide and are smaller than 3 km^2 in an R_{VA} landscape analysis of relative mountain front activity.

In summary, a measure of mean drainage basin depth, expressed as the ratio of eroded volume to planimetric area (R_{VA}) is an effective metric in determining the relative tectonic activity of fault-bounded mountain fronts and escarpments. When combined with other data, in this case the gradients of first-order streams, the R_{VA} can determine the relative position of a drainage basin along a time-dependent pathway (fig. 2). An important contribution of our study is that when plotted against the gradients of first-order streams, (fig. 6) real R_{VA} data confirm the theoretical plot of fig. 3, suggesting that drainage basins grow in a self-similar fashion, keyed into the size of the range that they are eroding and the rate of uplift. The R_{VA} alone in this case is an effective metric for determining relative tectonic activity of a mountain front undergoing rates of tectonic deformation like those observed in the Taos, Wasatch, and Black ranges. It is a less diagnostic metric for discerning tectonic activity when rates of rock uplift are low, as they are in Sierra Nacimiento, or when specific rock types and processes such as widespread earthflows work to keep basin slopes below the critical threshold angle for competent rock, as they do in the northern Apennines. Further testing of the R_{VA} will ultimately determine its utility in tectonic geomorphology, but the results we present here are promising and constitute an important step forward from the initial contributions stemming from the Bull & McFadden (1977) approach.

REFERENCES

ARMSTRONG P.A., TAYLOR A.R. & EHLERS T.A. (0000) - *Is the Wasatch Fault footwall (Utah, United States) segmented over million-year time scales?*. Geology, 32, 385-388.

BEAUMONT C., KOOI H. & WILLETT S. (2000) - *Coupled tectonic-surface process models with applications to rifted margins and collisional orogens*. In: Summerfield M. (ed.), «Geomorphology and Global Tectonics», John Wiley and Sons, Chichester, pp. 29-55.

BENEDETTI L.C., TAPPONNIER P., GAUDEMER Y., MANIGHETTI I. & VAN DER WOERD J. (2003) - *Geomorphic evidence for an emergent active thrust along the edge of the Po Plain. The Broni-Stradella fault*. Journal of Geophysical Research, 108, doi:10.1029/2001JB001546.

BIERMAN P. & CAFFEE M. (2001) - *Slow rates of rock surface erosion and sediment production across the Namib desert and escarpment, South Africa*. American Journal of Science, 301, 326-358.

BISHOP P. & GOLDRICK G. (2000) - *Geomorphologic evolution of the East Australia continental margin*. In: Summerfield M. (ed.), «Geomorphology and Global Tectonics», John Wiley and Sons, Chichester, pp. 225-254.

BOCCALETTI M., BONINI M., CORTI G., GASPERINI P., MARTELLI L., PICCARDI L., SEVERI P. & VANNUCCI G. (2004) - *Carta sismotettonica della Regione Emilia-Romagna e Note Illustrative*. Servizio Geologico, Sismico, e dei Suoli, Regione Emilia Romagna, 60 pp., scale 1:250,000.

BONNET S. & CRAVE A. (2003) - *Landscape response to climate change. Insights from experimental modeling and implications for tectonic versus climatic uplift of topography*. Geology, 31, 123-126.

BROWN R.W., SUMMERFIELD M.A. & GLEADOW A.J.W. (2002) - *Denudational history along a transect across the Drakensberg Escarpment of Southern Africa derived from apatite fission track thermochronology*. Journal of Geophysical Research, B, 107 pp.

BROWN R.W., GALLAGHER K., GLEADOW A.J.W. & SUMMERFIELD M.A. (2000) - *Morphotectonic evolution of the South Atlantic margins of Africa and South America*. In: Summerfield M.A. (ed.), «Geomorphology and Global Tectonics», John Wiley and Sons, Chichester, pp. 255-281.

BRYAN K. (1940) - *The retreat of slopes: Annals of the Association of American Geography*, 30, 254-268.

BRYANT B. (1990) - *Geologic map of the Salt Lake City 30' X 60' Quadrangle, north-central Utah and Uinta County, Wyoming*. United States Geological Survey Miscellaneous Investigations Series Map I-1944, scale 1:100,000.

BULL W.B. & MCFADDEN L.D. (1977) - *Tectonic geomorphology north and south of the Garlock fault, California*. In: Doehring D.O. (ed.), «Geomorphology of Arid Regions», Proceedings of the Eighth Annual Geomorphology Symposium, State University of New York at Binghamton, Binghamton, NY, 115-138.

BURBANK D.W., LELAND J., FIELDING E., ANDERSON R.S., BROZOVIC N., REID M.R. & DUNCAN C. (1996) - *Bedrock incision, rock uplift and threshold hillslopes in the northwestern Himalayas*. Nature, 379, 505-510.

CERRINA FERONI A., LEONI L., MARTELLI L., MARTINELLI P., OTTRIA G. & SARTI G. (2001) - *The Romagna Apennines, Italy: an eroded duplex*. Geological Journal, 36, 39-54.

CHANG W.L. & SMITH R.B. (2002) - *Integrated seismic-hazard analysis of the Wasatch front, Utah*. Bulletin of the Seismological Society of America, 92, 1904-1922.

COCKBURN H.A.P., BROWN R.W., SUMMERFIELD M.A. & SEIDL M.A. (2000) - *Quantifying passive margin denudation and landscape development using a combined fission-track thermochronology and cosmogenic isotope analysis approach*. Earth and Planetary Science Letters, 179, 429-435.

DENSMORE A.L., DAWERS N.H., GUPTA S. & GUIDON R. (2005) - *What sets topographic relief in extensional footwalls*. Geology, 33, 453-456.

DENSMORE A.L., DAWERS N.H., GUPTA S., GUIDON R. & GOLDIN T. (2004) - *Footwall topographic development during continental extension*. Journal of Geophysical Research, 109, doi, 10.1029/2003 JF000115.

DENSMORE A.L., ELLIS M.A. & ANDERSON R.S. (1998) - *Landsliding and the evolution of normal-fault-bounded mountains*. Journal of Geophysical Research, 103, 15, 203-15, 219.

FRANKEL K.L. (2002) - *Quantitative topographic differences between erosionally exhumed and tectonically active mountain fronts. Implications for late-Cenozoic evolution of the southern Rocky Mountains [M.S. Thesis]*. Bethlehem, Lehigh University, 138 pp.

FRANKEL K.L. & PAZZAGLIA F.J. (2006) - *Mountain fronts, base level fall, and landscape evolution. Insights from the southern Rocky Mountains*. In: Willett S., Hovius N., Brandon M. & Fisher D. (eds.), «Tectonics, climate, and landscape evolution», Geological Society of America Special Paper 398, in press.

GARCIA A.F., ZHU Z., KU T. L., SANZ DE GALDEANO C., CHADWICK O.A. & MONTERO J.C. (2003) - *Tectonically driven landscape development within the eastern Alpujarran Corridor, Betic Cordillera, SE Spain (Almería)*. Geomorphology, 50, 83-110.

GARDNER T.W., HARE P.W., PAZZAGLIA F.J. & SASOWSKY I.D. (1987) - *Evolution of drainage systems along a convergent plate margin, Pacific Coast, Costa Rica*. In: Graf W.L. (ed.), «Geomorphic systems of North America». The Geology of North America, Decade of North American Geology, Geological Society of America, special centennial volume 2, Boulder, Colorado, 357-372.

GILCHRIST A.R., KOOI H. & BEAUMONT C. (1994) - *Post-Gondwana geomorphic evolution of southwest Africa. Implications for the controls on landscape development from observations and numerical experiments*. Journal of Geophysical Research, 99, 12, 211-12, 228.

GLOCK W.S. (1931) - *The development of drainage systems and the dynamic cycle*. The Ohio Journal of Science, 31, 309-334.

HARBOR D.J. (1997) - *Landscape evolution at the margin of the Basin and Range*. Geology, 25, 1111-1114.

HASBARGEN L.E. & PAOLA C. (2000) - *Landscape instability in an experimental drainage basin*. Geology, 28, 1067-1070.

HAYMAN N.W., KNOTT J.R., COWAN D.S., NEMSER E.S., SARNA-WOJCICKI A.M. (2003) - *Quaternary low-angle slip on detachment faults in Death Valley, California*. Geology, 31, 343-346.

HOLM D.K. & DOKKA R.K. (1993) - *Interpretation and tectonic implications of cooling histories. An example from the Black Mountains, Death Valley extended terrane, California*. Earth and Planetary Science Letters, 116, 63-80.

HOLM D.K. & WERNICKE B. (1990) - *Black Mountains crustal section, Death Valley extended terrain, California*. Geology, 18, 520-523.

HOVIUS N. (1996) - *Regular spacing of drainage outlets from linear mountain belts*. Basin Research, 8, 29-44.

HUMPHREY N.F. & HELLER P.L. (1995) - *Natural oscillations in coupled geomorphic systems; an alternative origin for cyclic sedimentation*. Geology, 23, 499-502.

KING L.C. (1953) - *Canons of landscape evolution*. Geological Society of America Bulletin, 64, 721-752.

KLINGER R.E. & PIETY L.A. (2001) - *Holocene faulting and slip rates along the Black Mountains fault zone near Mormon Point*. In: Machette M.N., Johnson M.L. & Slate J.L. (eds.), «Quaternary and late Pliocene geology of the Death Valley region. Recent observations on tectonic, stratigraphy, and lake cycles». U. S. Geological Survey Open-File Report OF 01-0051, L193-L203.

KOOI H. & BEAMOUNT C. (1994) - *Escarpment retreat on high-level rifted plateau margins. Insights derived from a surface-process model that combines diffusion, reaction, and advection*. Journal of Geophysical Research, 99, 12, 191-12, 209.

LAGUE D., CRAVE A. & DAVY P. (2003) - *Laboratory experiments simulating the geomorphic response to tectonic uplift*. Journal of Geophysical Research, 108, doi, 10.1029/2002JB001785.

LIPMAN P.W. & REED J.C. JR. (1989) - *Geologic map of the Latir volcanic field and adjacent areas, northern New Mexico*. United States Geological Survey Miscellaneous Investigations Series Map I-1907, scale 1:48,000.

MACHETTE M.N., PERSONIOUS S.F., NELSON A.R., SCHWARTZ D.P. & LUND W.R. (1991) - *The Wasatch fault zone, Utah - Segmentation and history of Holocene earthquakes*. Journal of Structural geology, 13, 137-149.

MATMON A., BIERMAN P. & ENZEL Y. (2002) - *Pattern and tempo of great escarpment erosion*. Geology, 30, 1135-1138.

MATTSON A. & BRUHN R.L. (2001) - *Fault slip rates and initiation age based on diffusion equation modeling. Wasatch Fault Zone and eastern Great Basin*. Journal of Geophysical Research, 106, 13, 739-13, 750.

MENGES C.M. (1990a) - *Late Quaternary fault scarps, mountain front landforms, and Pliocene-Quaternary segmentation on the range-bounding fault zone, Sangre de Cristo Mountains, New Mexico*. In: Krinitzsky E.L. & Slemmons D.B. (eds.), «Neotectonics in earthquake evaluation». Boulder, Colorado, Geological Society of America Reviews in Engineering Geology, 8, 131-156.

MENGES C.M. (1990b) - *Soils and geomorphic evolution of bedrock facets on a tectonically active mountain front, western Sangre de Cristo Mountains, New Mexico*. Geomorphology, 3, 301-332.

MERRITTS D.J. & VINCENT K.R. (1989) - *Geomorphic response of coastal streams to low, intermediate, and high rates of uplift, Mendocino triple junction region, northern California*. Geological Society of America Bulletin, 100, 1373-1388.

MONTGOMERY D.R. & BRANDON M.T. (2002) - *Topographic controls on erosion rates in tectonically active mountain ranges*. Earth and Planetary Science Letters, 201, 481-489.

MORISAWA M.E. (1964) - *Development of drainages systems on an upraised lake floor*. American Journal of Science, 262, 340-354.

OLLIER C.D. (1985) - *Morphotectonics of continental margins with Great Escarpments*. In: Morisawa M. & Hack J.T. (eds.), «Tectonic Geomorphology», Binghampton Symposium in Geomorphology. International Series, 15, 3-25.

OUCHI S. & MATSUSHITA M. (1997) - *Morphological characteristics and evolution of miniature erosional landforms generaled by artificial rainfall*. Journal of the Institute of Science and Engineering, Chuo University, 3, 67-80.

PARKER R.S. & SCHUMM S.A. (1982) - *Experimental study of drainage networks*. In: Bryan R. & Yair A. (eds.), «Badland geomorphology and piping». Norwich, Geobooks, 153-168.

PAZZAGLIA F.J. (1989) - *Tectonic and climatic influences on the evolution of Quaternary depositional landforms along a segmented range-front fault, Sangre de Cristo Mountains, north-central New Mexico [M.S. Thesis]*. Albuquerque, University of New Mexico, 246 pp.

PAZZAGLIA F.J. & BRANDON M.T. (1996) - *Macrogeomorphic evolution of the post-Triassic Appalachian mountains determined by deconvolution of the offshore basin sedimentary record*. Basin Research, 8, 255-278.

PAZZAGLIA F.J. & KELLEY S.A. (1998) - *Large-scale geomorphology and fission-track thermochronology in topographic and exhumation reconstructions of the southern Rocky Mountains*. In: Karlstrom K. (ed.), «Lithospheric evolution of the Rocky Mountains». Rocky Mountain Geology, 33, 229-257.

PIKE R.J. & WILSON S.E. (1971) - *Elevation-relief ratio, hypsometric integral, and geomorphic area-altitude analysis*. Geological Society of America Bulletin, 82, 1079-1084.

REGIONE EMILIA-ROMAGNA, SERVIZIO METEOROLOGICO REGIONALE (1995) - *I numeri del Clima: temperature, precipitazioni e vento*. Tavole climatologiche dell'Emilia-Romagna 1951-1994, Promodis Italia, Brescia.

RITTER J.B. & GARDNER T.W. (1993) - *Hydrologic evolution of drainage basins disturbed by surface mining, central Pennsylvania*. Geological Society of America Bulletin, 105, 101-115.

ROCKWELL T.K., KELLER E.A. & JOHNSON D.L. (1985) - *Tectonic geomorphology of alluvial fans and mountain fronts near Ventura, California*. In: Morisawa M. & Hack J.T. (eds.), «Tectonic geomorphology», Binghamton Symposia in Geomorphology. International Series, 15, 183-207.

ROERING J.J., KIRCHNER J.W. & DIETRICH W.E. (1999) - *Evidence for nonlinear, diffusive sediment transport on hillslopes and implications for landscape morphology*. Water Resources Research, 35, 853-870.

ROERING J.J., KIRCHNER J.W., SKLAR L.S. & DIETRICH W.E. (2001) - *Hillslope evolution by nonlinear creep and landsliding. An experimental study*. Geology, 29, 143-146.

SCHUMM S.A., MOSLEY M.P. & WEAVER W.E. (1987) - *Experimental fluvial geomorphology*. John Wiley and Sons, New York, 413 pp.

SCHWARTZ D.P. & COPPERSMITH K.J. (1986) - *Seismic hazards; new trends in analysis using geologic data*. In: Wallace R.E. (ed.), «Active tectonics», National Academy of Science Press, Washington, D.C., 215-230.

SPAGNOLO M. & PAZZAGLIA F.J. (2005) - *Testing the geological influences on the evolution of river profiles: a case from the Northern Apennines (Italy)*. Geografia Fisica e Dinamica Quaternaria, 28, 103-113.

STRAHLER A.N. (1952) - *Hypsometric (area-altitude) analysis of erosional topography*. Geological Society of America Bulletin, 63, 1117-1142.

TUCKER G.E. & SLINGERLAND R.L. (1994) - *Erosional dynamics, flexural isostasy, and long-lived escarpments. A numerical modeling study*. Journal of Geophysical Research, 99, 12, 229-12, 243.

VAN DER BEEK P., SUMMERFIELD M.A., BRAUN J., BROWN R.W. & FLEMING A. (2002) - *Modeling postbreakup landscape development and denudational history across the southeast African (Drakensberg Escarpment) margin*. Journal of Geophysical Research, 107, doi, 10.1029/2001JB000744.

WELLS S.G., BULLARD T.F., MENGES C.M., DRAKE P.G., KARAS P.A., KELSON K.I., RITTER J.B. & WESLING J.R. (1988) - *Regional variations in tectonic geomorphology along a segmented convergent plate boundary, Pacific coast of Costa Rica*. Geomorphology, 1, 239-265.

WOODWARD L.A. (1987) - *Geology and mineral resources of Sierra Nacimiento and vicinity, New Mexico*. New Mexico Bureau of Mines and Mineral Resources, Memoir 42, 84 pp.

ZAPROWSKI B.J., EVENSON E.B., PAZZAGLIA F.J. & EPSTEIN J.B. (2001) - *Knickzone propagation in the Black Hills and northern High Plains; a different perspective on the late Cenozoic exhumation of the Laramide Rocky Mountains*. Geology, 29, 547-550.